ELSEVIER

Journal of Neuroscience Methods 117 (2002) 13–21

JOURNAL OF NEUROSCIENCE METHODS

www.elsevier.com/locate/jneumeth

Extracellular potentials in low-density dissociated neuronal cultures

Enric Claverol-Tinture *, Jerome Pine [1]

Department of Physics, Mathematics and Astronomy, California Institute of Technology, 326 Kerchoff MC 156-29, 1200 East California Blvd., Pasadena, CA 91125, USA

Received 14 January 2002; received in revised form 1 March 2002; accepted 4 March 2002

Abstract

The detection of extracellular potentials by means of multi-electrode arrays (MEA) is a useful technique for multi-site long-term monitoring of cultured neuronal activity with single-cell resolution. To optimize the geometry of the MEA it is advantageous to localize the cellular compartments that constitute the generators of these signals. For this purpose, an in vitro technique for the detection of extracellular signals with subcellular resolution has been developed. It makes use of easy-to-manufacture large-tip pipettes, monitoring of electrode-cell gap resistance for precise electrode positioning and low-density (100 cells/mm^2) dissociated hippocampal cultures. Negative monophasic extracellular spikes, typically 60 μV, were measured over putative axonal processes and monophasic, biphasic and triphasic signals were recorded over the soma. A compartmental simulation suggests that different somatic conductance densities of Na^+ (1–10 mS/cm^2) and K^+ (5–10 mS/cm^2) channels can produce characteristic somatic extracellular potentials, with a variety of shapes similar to those observed experimentally.

Keywords: Extracellular potentials; Cultured hippocampal neurons; Multi-electrode arrays; Axon-hillock; Compartmental simulation; Neuron model

1. Introduction

In vivo and in vitro preparations are often combined with extracellular recordings to achieve stimulation and measurement of single cell and population activity (Drake et al., 1988; Oka et al., 1999; Nadásdy et al., 1999; Quirk et al., 2001). Multi-electrode arrays (MEA) combined with dissociated neuronal cultures are particularly promising as tools for the long-term study of network dynamics (Pine, 1980; Regehr et al., 1989; Zeck and Fromherz, 2001) since it is, in principle, possible to achieve two-way interaction with every neuron in a circuit. Despite the large body of literature on MEAs, there is little data to guide their design, i.e. how the geometrical relationship between neurons and electrodes affects the magnitude and sign of extracellularly recorded action potentials.

Extracellular potentials can be fully explained with well established biophysical principles of neural excitability (Nuñez, 1981; Holt and Koch, 1999). Ionic currents associated with action potentials and subthreshold activity flow in closed loops. The components relevant to the genesis of extracellular potentials enter the neuron at current sink regions, propagate through the cytosolic medium, leave it at current source regions and return to the sink points through the extracellular space. Spatio-temporal patterns of extracellular voltages appear as a result of this return current.

The identification of the neuronal compartments responsible for the observed extracellular signals (i.e. localization of sinks and sources) is a prerequisite in order to determine the MEA geometry that optimizes network–MEA interaction. The size and arrangement of the electrodes could then be set to maximize the probability of any given cell having its largest intensity current sources and sinks close to recording electrodes. Alternatively, once the cellular compartments capable of generating largest extracellular potentials are identified, the position of the neurons might be physically constrained (Maher et al., 1999), or the growth of processes

* Corresponding author. Tel.: +1-626-395-6787; fax: +1-626-564-8708.

E-mail addresses: enric@caltech.edu (E. Claverol-Tinture), jpmail@caltech.edu (J. Pine).

[1] Tel.: +1-626-395-6677; fax: +1-626-564-8708.

0165-0270/02/$ - see front matter
PII: S0165-0270(02)00043-2

along convenient paths could be chemically promoted (Branch et al., 2000; James et al., 2000), to ensure efficient neuron–MEA interaction.

Although the localization of the extracellular potential generators has been tackled theoretically (Rall, 1969), the unknown spatial distribution of active channels limits the usefulness of theoretical predictions. Sink and source localization can be studied experimentally, by mapping the spatio-temporal distribution of extracellular potentials using movable microelectrodes or fixed arrays. In this way, current density analysis in vivo and in slice preparations (Nicholson and Freeman, 1975; Novak and Wheeler, 1989; Ketchum and Haberly, 1993) provides macroscopic information on extracellular current flow. These preparations are particularly suitable for extracellular recording. Firstly, the reduced extracellular space due to the compact arrangements of neurons and glia increases the effective resistance through which extracellular currents circulate, causing easily detectable potential differences (i.e. in the order of 100 μV). Secondly, the high density of neurons also maximizes the probability of an electrode being close to a sufficiently intense current source or sink.

The application of MEAs to microcircuit studies requires, however, the use of low density dissociated cultures, because networks with reduced anatomical complexity facilitate monitoring and stimulation of individual neurons. Unfortunately, current density analysis data from non-dissociated tissue is difficult to extrapolate to dissociated cultures in order to predict the optimum MEA electrode arrangement. Therefore, mapping of the spatio-temporal patterns of extracellular potentials must be carried out to study recording in dissociated cultures.

These sparse cultures pose problems to the mapping of extracellular potentials with movable microelectrodes because the open extracellular space, free of electrical insulation due to lack of surrounding cells, acts as a low resistance path from current sources to current sinks, reducing the resulting potentials compared to those measured under the tightly packed geometries found in vivo. Moreover, in vivo, the probability of a randomly positioned electrode falling within a few micrometers of a current source is high due to the high cell density but extracellular recordings in vitro are expected to call for positioning of the electrodes at short distances from current sinks or sources. For this purpose, a reliable method is required to measure electrode-cell distances of the order of micrometers in the axis perpendicular to the plane occupied by the culture.

This paper describes a technique to measure spatio-temporal maps of extracellular potentials generated by individual neurons in dissociated cultures using a movable glass microelectrode. Precise positioning is achieved by monitoring of the pipette-cell gap resistance. The technique allows the identification of current sources and sinks along processes and over cell somas. A compartmental model is also presented to aid the interpretation of the experimental data and implications for MEA design are discussed.

2. Methods

2.1. Cell culture

Low-density cultures of dissociated embryonic rat hippocampal neurons were prepared as has been described (Banker and Goslin, 1998). Briefly, hippocampi were removed from E18 and E19 embryonic rats, dissociated with trypsin for 15 min at 37 °C and gently triturated. The cells were plated on poly-L-lysine-coated 35-mm plastic Petri dishes at a density of 100 cells/mm^2. The plating medium was MEM (Minimum Essential Medium, GIBCOBRL 11095-080) supplemented with 10% F12 (GIBCOBRL 11765-054) and 10% equine serum. Cytosine β-D-arabino furanoside (Sigma) was added at 1 μM 1 week after plating to inhibit glial proliferation. Cells were studied after 12–16 days in culture when neurons and a thin glial carpet were present.

2.2. Extracellular recordings

Pipettes with large tips (ID = 10–20 μm) and wall thickness at the tip of approximately 6 μm were pulled from borosilicate glass capillaries (Sutter BF150-86-110, ID = 0.86 mm, OD = 1.5 mm) using standard equipment (Sutter Instruments P-97). The pulling process involved 5–7 pulling cycles and variability in tip sizes resulted in a low (approximately 20%) yield of usable electrodes. Thick pipette walls (> 5 μm) were desirable to achieve measurable electrode-dish gap resistances in order to monitor electrode-cell distance, as described below. Typical pipette resistances were 50–200 kΩ when filled with bath solution (in mM): 145 NaCl, 3 KCl, 5 $CaCl_2$, 8 glucose and 10 HEPES (pH 7.3).

Upon identification of an isolated cell with clearly visible processes, the pipette was manually positioned vertically with respect to the plane of the cell culture and lowered using a mechanical manipulator (Leitz) to approach the process or soma from which extracellular signals were sought. The pipette resistance was monitored continuously by injecting 10 ms pulses of 100 nA and simultaneously measuring the voltage at the electrode with a custom made amplifier in current-clamp mode (Fig. 1A).

Upon detection of a 10–20 kΩ increase in apparent pipette resistance, the approaching phase was terminated. Visual inspection indicates that, at this point, the electrode is located at approximately 5 μm above the culture dish, so that the increase in measured resistance

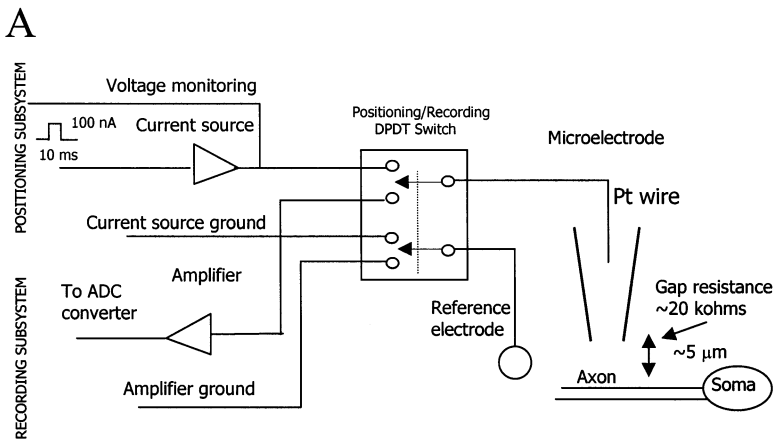

B

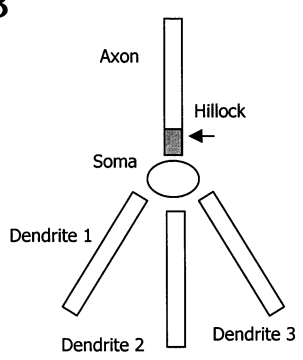

General Parameters			
Time step	2 µs	Intrac. Res.	1 ohm x m
Capacitance	1 µF/cm²	Gleak	0.1 mS / cm²
ENa	50 mV	EK	-70 mV
Eleak	- 60 mV		
Soma			
Radius	10 µm	GNa	1-10 mS/ cm²
GK	5-10 mS/ cm²	Stim.	750 pA
Axon			
# compart.	100	Radius	1.5 µm
Length	2 mm	GNa Hillock	50 mS/ cm²
GK Hillock	50 mS/ cm²	Hillock length	60 µm
Dendrites (3)			
# compart.	100	Radius	1 µm
Length	2 mm	GNa	0 mS/ cm²
GK	0 mS/ cm²		

Fig. 1. (A) Setup for electrode positioning (current source and voltage monitor) and extracellular recording (low-noise amplifier) and interconnection by DPDT switch. (B) Sketch of the compartmental model and parameter set.

can be attributed to the thin film of bath solution under the edge of the pipette (gap resistance). Having positioned the electrode, the double-pole double-throw (DPDT) switch was actuated to disconnect the positioning subsystem (resistance monitoring) and connect the extracellular recording amplifier to the electrode and a reference wire.

A custom built low-noise differential amplifier based on the design by Chien and Pine (1991) was utilized with a low-pass filter (cutoff frequency at 5 kHz). Signals were digitized at 20 K samples/s and further filtered digitally for noise reduction with a cut-off frequency of 3 kHz. The noise level for a typical 100 kΩ electrode was 4 μV_{rms}. Finally, 60 Hz pickup interference was substracted by software when necessary.

Since 2-week-old cultures produce spontaneous activity, often in bursts, stimulation was not necessary. It was confirmed, however, that 1 ms negative pulses of 1 µA were sometimes successful at eliciting bursts of spikes on putative axons. Lack of activity after a 5 min recording phase waiting for spontaneous firing, prompted stimulation tests, and, eventually, repositioning to a new process or cell. This procedure was iterated until activity was detected.

2.3. Intracellular recordings

Whole-cell perforated patch recordings (Rae et al., 1991), using amphotericin B (150 µg/ml, Calbiochem) were carried out on selected cells to confirm the neuronal origin of the extracellular potentials. The pipettes were pulled from borosilicate glass capillaries (Sutter BF150-86-110) and resistances were in the range 1–5 MΩ. The internal solution contained (mM): 136.5 Kgluconate, 17.5 KCl, 1 $MgCl_2$, 10 HEPES and 0.2 EGTA (pH 7.3).

2.4. Compartmental model

A compartmental model was created using standard techniques (Koch and Segev, 1998) with Matlab (Mathworks) to confirm that realistic cell geometries and channel densities were consistent with the measured extracellular signals. The model included a spherical soma, three dendrites and a single axon (see Fig. 1B and inset table for a complete parameter set). The geometry of the model was akin to a cultured triangular cell and typical physiological values were used to describe passive and active membrane characteristics. The dynamics of the Na^+ and K^+ active channels were modeled using the Hodgkin–Huxley formalism (Hodgkin and Huxley, 1952) with parameters taken from Traub et al. (1991).

Dendrites were assumed passive while the soma and the 60 μm proximal axonal segment (axon-hillock, AH) were populated with Na^+ and K^+ channels with Hodgkin–Huxley dynamics and conductance densities: $GNa_{soma} = 1–10$ mS/cm^2, $GK_{soma} = 5–10$ mS/cm^2, $GNa_{AH} = 50$ mS/cm^2, $GK_{AH} = 50$ mS/cm^2. The transmembrane current associated with an action potential in the model was used to estimate the extracellular potential recorded by an electrode positioned close to the process or soma:

$$V(t) = I(t) \times R_{gap}, \quad (1)$$

where $I(t)$ is the total transmembrane current in the patch of membrane under the recording electrode and R_{gap} takes a value of 20 kΩ, corresponding to the measured resistance between pipette core and extracellular medium (gap resistance).

3. Results

3.1. Cell-electrode gap

Upon positioning of the pipette at approximately 5 μm from the Petri dish, gap resistances of 10–20 kΩ between the core of the pipette and the extracellular space were readily obtained. An analytical expression can be derived to provide a rough estimate for the resistance of the restricted volume of conductive medium under the edges of the pipette. Assuming that the current flows radially in a corona of saline (the space between the edge of the pipette and the Petri dish), the gap resistance is given by,

$$R_{gap} = (\rho/2\pi r) \times \ln \mathrm{OD/ID}, \quad (2)$$

where ρ is the resistivity of the medium (typically 0.5 Ωm), r the distance between pipette and dish (thickness of saline annulus) and OD and ID are the outer and inner diameters of the pipette. For values of $r = 5$ μm and OD = 30 μm and ID = 15 μm, R_{seal} takes a value of 11 kΩ, as typically measured in our experiments.

Note that this is a rough approximation and numerical solutions would be needed to account for the geometry of the problem. Expression 2 provides a lower limit for the resistance encountered by current flowing from the core of the pipette to the reference electrode since a second component, accounting for the spread resistance from the edge of the annulus, would add to the gap resistance. Expression 2 provides, nevertheless, a semi-quantitative view of the electrical effect of the close pipette-cell positioning.

Rough pipette edges, which were sometimes seen after pulling, produced gap resistances at the low end of the range whereas cleanly cut tips, presumably positioned at $r < 5$ μm, occasionally achieved resistances up to 30 kΩ without physical contact with the dish.

3.2. Neuronal origin of extracellular signals

Two tests were carried out to confirm the neuronal origin of the recordings: simultaneous whole-cell and extracellular recordings, and validation of signal size dependence on vertical (normal to culture plane) cell-electrode distance and horizontal (coplanar with the culture) electrode position. For the experiment shown in Fig. 2A, the patch pipette was positioned to occupy one half of the visible somatic surface and the extracellular electrode was positioned above the other half. Fig. 2A shows an extracellular biphasic recording (upper trace) and simultaneous whole-cell recording (lower trace). Further confirmation of the neuronal origin of the extracellular signals was obtained by studying the dependence of the magnitude of the extracellular spikes with respect to cell-electrode distance. Fig. 2B shows the peak value of axonal negative monophasic spikes obtained on a single putative axon as a function of cell-electrode gap resistances. Increasing resistances were achieved as the gap narrows during vertical approach, confirming that the distance between cell and electrode affects signal size as expected if the latter was the signal source.

Moreover, lateral displacements of the electrode should also affect signal size. Fig. 2C shows signals recorded at six locations, including the soma of a triangular cell. The dotted lines indicate the limits of the internal perimeter of the pipette (ID = 18 μm). The rightmost positions cover an area with several processes, probably including the axon from the triangular cell at the center of the image. Consistent with axonal recordings, negative peaks were clearly seen at these locations. The leftmost area corresponds to a process-free region, where characteristic axon spikes cannot be recorded.

Further, the time course of the negative spikes above processes, with typical half-height durations of 500 μs, as well as the presence of bursts with 5–10 spikes, are

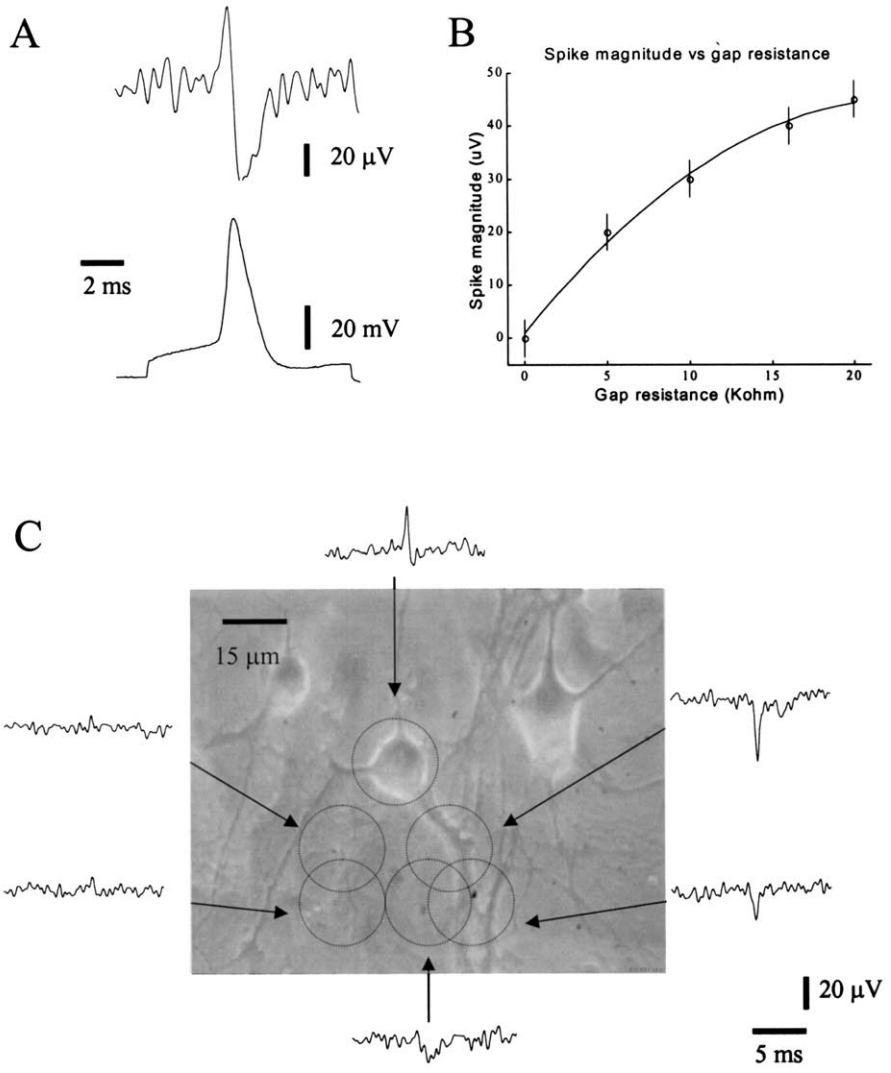

Fig. 2. (A) Simultaneous whole-cell and somatic extracellular recording. (B) Extracellular spike size, recorded on an axon, as a function of gap resistance. (C) Dependence of spike shape and magnitude on electrode position with respect to processes and soma.

consistent with neuronal activity. Having confirmed the neuronal origin of the extracellular signals, recordings from 42 neurons were carried out, both from soma and processes. In each case, only a subset of the visible processes were selected, those unequivocally originating from the chosen cell.

3.3. Somatic signals

Upon achievement of gap resistances of 10–20 kΩ, recordings over somas could be obtained. Fig. 3A shows four examples from different cells, the main characteristic being the variability of the magnitude and shape across cells. Multiphasic signals (positive–negative or positive–negative–positive) were recorded in 58% of the somatic recordings. Monophasic negative and monophasic positive were obtained in 33 and 9% of the neurons, respectively.

3.4. Dendritic and axonal signals

Only 30% of the processes produced signals above noise level; 26% produced large (typically 40–60 μV) monophasic negative peaks and 4% produced low-magnitude (approximately 10 μV) monophasic positive spikes. The former were assumed to be putative axons and the latter, along with recordings without signals above noise, were assumed to be dendrites. Axonal recordings were achieved at distances from 20 to 50 μm from the soma. Measurements from locations further away than 50 μm were not routinely made due to the presence of other neurons and loss of visual access to the process under the glial carpet or within the network of processes. Two axonal recordings from two different cells are shown in Fig. 3B. The magnitude of the negative spike on axons varied across cells, typically within the 40–60 μV range.

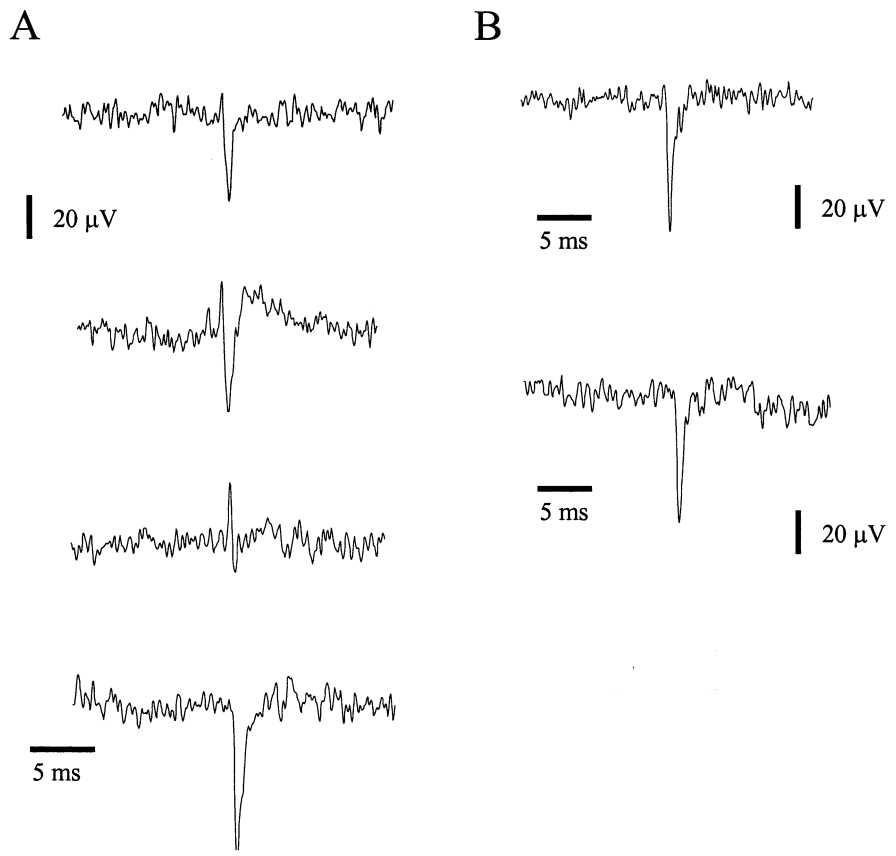

Fig. 3. Extracellular potentials over cell somas (A) and axons (B).

3.5. Simulation results

The compartmental model was used to compare theoretical and experimental extracellular potentials. Fig. 4 shows simulations with three different somatic concentrations of Na^+ and K^+ channels; high excitability (although low compared to the axon, labeled HE), GNa = 10 mS/cm^2 and GK = 5 mS/cm^2, medium excitability (ME), GNa = 5 mS/cm^2 and GK = 10 mS/cm^2 and low excitability (LE), GNa = 1 mS/cm^2 and GK = 5 mS/cm^2. The remaining parameters were not changed.

In all models, somatic current injection (750 pA) triggered action potentials. Fig. 4A shows intracellular action potentials at the soma. Note that the action potential in the HE model peaks 300 μs before that in the ME, consistent with higher somatic excitability.

Fig. 4B–D show the predicted extracellular signals over the axon-hillock, dendrites and soma, respectively. They were derived, as described in Section 2, from the transmembrane currents, applying Eq. (1) and assuming a gap resistance of 20 kΩ. Fig. 4B shows how fast-activating Na^+ channels in the axon-hillock are capable of generating negative peaks of 70–80 μV followed by a 25 μV positive peak due to K^+ driven repolarization. Fig. 4C shows that, in all cases, dendritic signals have low magnitude 15 μV peak-to-peak and a biphasic positive–negative shape. The initial positive phase is generated by the dendritic current source resulting from passive propagation from the soma to the proximal dendritic compartments and to the extracellular space through the dendritic membrane. During repolarization, this current reverses, causing the negative phase. Fig. 4D shows how soma excitability affects the shape of somatic extracellular recordings. The HE parameter set (GNa = 10 mS/cm^2) predicts a single negative peak which occurs simultaneously with the axonal spike. The ME model (GNa_{soma} = 5 mS/cm^2 and GK_{soma} = 10 mS/cm^2) predicts a triphasic signal. The initial positive phase is caused by the outward capacitive current at the soma which occurs as the axon current sink peaks. As the axonal action potential starts repolarizing, this current (a positive contribution) decreases and the inward current from the Na^+ channels present in the soma dominates the total transmembrane current. Finally, the slowly inactivating K^+ channels repolarize the somatic membrane causing a third (positive) phase. The LE (GNa_{soma} = 5 mS/cm^2) model includes a nearly passive soma which shows a transmembrane current with a similar shape to the totally passive proximal dendritic segment. Both the positive and negative phases are due to return currents from the axon.

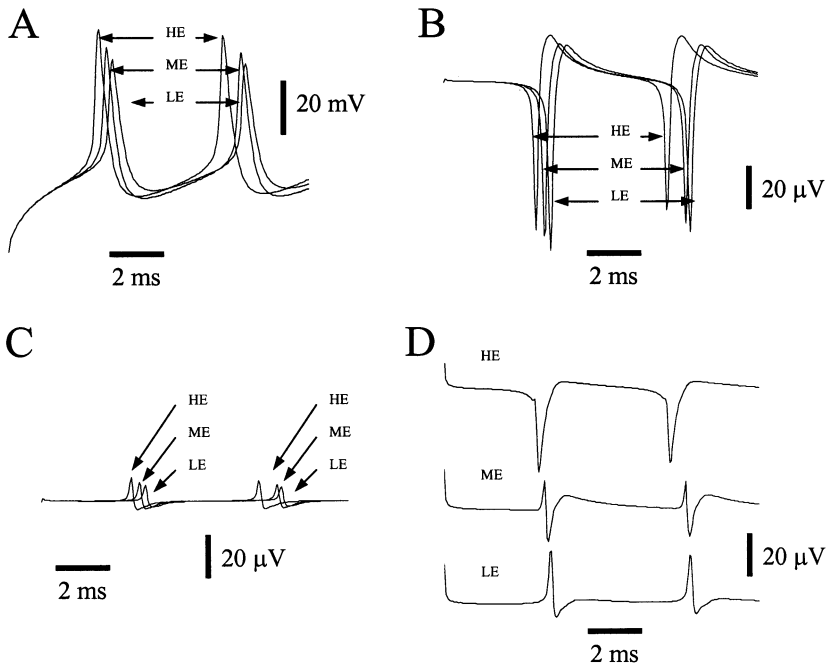

Fig. 4. (A) Simulated intracellular action potentials upon somatic injection of 750 nA. Simulation results for various values of somatic GNa (high, 10 mS/cm^2, medium, 5 mS/cm^2, and low, 1 mS/cm^2, somatic excitability). Predicted extracellular spikes above the axon (B), dendrites (C) and soma (D) at $R_{gap} = 20$ kΩ.

4. Discussion

This paper extends previous work on in-vivo single-unit extracellular potentials recorded with silicon probes (Drake et al., 1988) to an in-vitro preparation which allows visual control of the position of the neuron relative to the electrode. Measurements of extracellular potentials from identified neuronal compartments in low-density cultures have been achieved by positioning a large pipette at a short distance (approximately 5 μm) from the bottom of the culture dish in order to achieve a gap resistance of 10–20 kΩ. Simultaneous intracellular and extracellular recordings in addition to studies of signal size dependence on cell-electrode distance confirmed the neuronal origin of the recorded signals. The shape (monophasic negative and biphasic/triphasic), magnitude (40–60 μV on the axon) and duration (typically 500 μs) are also consistent with previous work on extracellular recordings.

The compartmental model confirms that the axon-hillock is capable of generating extracellular negative peaks of 60 μV in amplitude whereas passive dendrites are expected to produce low amplitude (<10 μV) positive peaks. The model also suggests that the shape and magnitude of the somatic extracellular signals are dependent on the density of somatic Na^+ channels. Values in the order of 1 mS/cm^2 produce positive extracellular peaks while 10 mS/cm^2 result in negative axon-like peaks.

Overall, the presented technique, and the results that derived from it, match a classical view of action potential generation. A subset of the cellular processes generated recordable signals, when clearly above noise (40–60 μV) always of the monophasic negative type. This subset was assumed to correspond to axons which act as current sinks and are responsible for the Na^+ influx needed for depolarization. A second group of processes did not generate clear signals above noise. It was confirmed that neurons with clearly detectable spontaneous negative spikes on putative axons did not generate detectable signals on the remaining processes. Moreover, sometimes, low magnitude (10 μV) positive peaks could be detected on these processes while a clear 60 μV negative peak was detectable on the axon. It was concluded that they were dendrites and that the lack of signals was due to the low magnitude of the potentials created by outward dendritic currents during action potential generation. It can be expected that the magnitude of the recorded spike would increase if a loose-patch configuration was to be used, since the physical contact between electrode and dendritic membrane would result in higher seal resistance. Such an experimental paradigm is, however, of limited relevance for MEA technology since seal of a microfabricated electrode to a dendrite is in general difficult to achieve.

Recordings over somas are complex. Positive peaks can be explained considering the soma as a large passive dendritic segment whose surface (1256 μm^2 for a 10 μm radius) and associated capacitance (12.6 pF) act as a low impedance path for outward current from the axon. To further quantify this idea, consider an axon sinking current from the extracellular medium and injecting a

fraction of it into the soma to achieve a prototypical action potential with a (standard) rising phase of 100 mV/ms. For a 12.6 pF somatic capacitance, the capacitive outward current would be 1.26 nA ($C \times dV/dt$), recorded as a 25.2 μV positive peak by an electrode positioned over the soma with a gap resistance of 20 kΩ. Preliminary loose-patch somatic recordings (pipette tip ≈3 μm, pipette resistance = 1 MΩ, seal resistance = 10 MΩ) have confirmed that the main component of the somatic current is capacitive and shows as a positive peak (outgoing current), followed by a negative phase (inward current).

Negative peaks recorded on somas may result from active channels, as shown by the model. However, since typical cells have a diameter of 15–20 μm, it is also possible that the internal diameter of the recording pipette exceeds that value, resulting in proximal segments of the axon contributing to somatic recordings. Further studies correlating electrode diameter, cell geometry and somatic signal shapes would be interesting in this respect. This also applies to the multi-phasic somatic recordings, which can be simulated adjusting the density of active channels in the soma but may also be influenced by the inclusion of portions of the axon or dendritic active channels (excluded in the presented model).

The ability to record extracellular potentials from localized cellular compartments allows rough estimations of transmembrane currents and channel densities. Consider an axonal spike of 60 μV recorded over an axon. It follows that, assuming a gap resistance of 15 kΩ, the total current flowing under the electrode is 4 nA (4 nA × 5 kΩ = 60 μV). The current density that corresponds to 4 nA flowing through a segment of axon covered by the electrode (say 30 μm in length, 1 μm in radius and, hence, 189 μm^2 of area) is 21 $pA/\mu m^2$. A similar calculation for the soma yields a current density of 2.8 $pA/\mu m^2$, obtained considering the area under the electrode to be a circular patch of radius 15 μm and taking the extracellular signal to be 30 μV.

Previous work using loose-patch recording from soma and axons of pyramidal cells in slices produced similar values for the soma (Colbert and Johnston, 1996). However, in the same work, current densities at proximal segments of the axon were found to be as low as in the soma, suggesting that the site of initiation of action potentials is actually located further away along the axon. Simulations by others (Rapp et al., 1996) have shown that this would require extremely high densities of Na^+ channels (40 times higher than somatic densities) in order to achieve normal action potentials. The results contained in this paper seem to indicate that, at least in vitro, the density of Na^+ channels in the proximal segment of the axon is 10-fold the somatic density and the simulations carried out show that this is sufficient for the generation of action potentials. In any case, by means of the presented extracellular technique, current densities can be mapped along the axon in vitro and the standing issue of the localization of the action potential generator can be tackled.

4.1. Limitations of the technique

Although clear extracellular signals were detected from 42 neurons, this represents approximately 50% of the attempted cells. This lack of signals may be due to low spontaneous firing rates in those cells. Even though stimulation was tested in these cases, only activity triggered in the form of long-lasting bursts can be observed with the currently used setup since the stimulation artifact and the manual switching time (from stimulation to recording) blanks out the first 100 ms after stimulation.

A solution would be to integrate stimulation and recording with artifact suppression circuitry and electronic switch between stimulation and recording modes as proposed by Barbour and Isope (2000) for the loose-patch configuration. Assuming that the stimulation artifact could be completely eliminated, silent neurons that would respond with single spikes to stimulation could then be detected. An alternative would be artifact-free pharmacological stimulation, for example local puffs of glutamate or KCl solutions (Maher et al., 1999). Simultaneous whole-cell stimulation and extracellular recording is possible. The drawbacks of this approach are, firstly, that screening of many cells would be time consuming and, secondly, that extracellular recordings would only be possible from a subset of the processes due to the space occupied by the patch pipette.

The glial carpet may act as an insulator between electrode and neuronal current sources. After 2 weeks in culture, a thin layer of glia covers the bottom of the dish. However, the processes and soma appear to rest on top of this layer, an observation that appears to be confirmed by preliminary electron-microscopy studies by others (Gross, 1994). Only when the density of glial cells reaches confluency, some neuronal processes seem to be partially covered by the glial carpet. Further experiments will be necessary to determine which of these factors, if not a combination, are responsible for silent cells.

5. Conclusions: implications for MEA technology

The ability to locally measure extracellular potentials has important consequences for the design of silicon–neuronal interfaces. The measurements that are possible with the proposed technique aid in the optimization of the dimensions and distribution of electrodes in MEA, by relating cellular compartments and extracellular potentials. The results already obtained suggest that Eq. (1)

large signals (occasionally up to 80 μV) can be recorded in dissociated cultures upon positioning of the recording electrode close (several micrometers) to an axon, and that Eq. (2) physical contact between electrode and membrane is not necessary. These two conclusions complement the existing knowledge that good seals between electrodes and somas result in large signals (Grattarola and Martionoia, 1993; Bove et al., 1995). Our results suggest that large monophasic negative peaks can also be recorded close to axons with no seal involving physical contact between electrode and cell. This is, in our experience, the most common shape recorded with planar MEAs. Hence, an alternative to physical confinement of neuronal somas on MEA electrodes by means of 3D structures, in order to achieve good seals (see Zeck and Fromherz, 2001), would be to provide a high enough density of electrodes or to use patterned surfaces to guide axonal outgrowth. In this way, the probability of having electrodes under or close to axons is maximized. Future work to test the feasibility of this approach would require MEAs with short inter-electrode distances in combination with low-density cultures that facilitate visual identification of processes and their relative positions with respect to the electrodes.

Acknowledgements

We thank the reviewers for their comments. We thank Axel Blau, Tom Demarse, Steve Potter and Daniel Wagenaar for useful discussions. This work was supported by NIH-SBIR grant R44NS037968-02.

References

Banker G, Goslin K. Culturing Nerve Cells. Cambridge: MIT Press, 1998.

Barbour B, Isope P. Combining loose cell-attached stimulation and recording. J Neurosci Methods 2000;103:199–208.

Bove M, Grattarola M, Martionoia S, Verreschi G. Interfacing cultured neurons to planar substrate microelectrodes: characterization of the neuron-to-microelectrode junction. Bioelectrochem Bioener 1995;38:255–65.

Branch DW, Wheeler BC, Brewer GJ, Leckband DE. Long-term maintenance of patterns of hippocampal pyramidal cells on substrates of polyethylene glycol and microstamped polylysine. IEEE Trans Biomed Eng 2000;47(3):290–300.

Chien CB, Pine J. An apparatus for recording synaptic potentials from neuronal cultures using voltage-sensitive fluorescent dyes. J Neurosci Methods 1991;38(2–3):93–105.

Colbert CM, Johnston D. Axonal action-potential initiation and Na+ channel densities in the soma and axon initial segment of subicular pyramidal neurons. J Neurosci 1996;16(21):6676–86.

Drake KL, Wise KD, Farraye J, Anderson DJ, BeMent SL. Performance of planar multisite microprobes in recording extracellular single-unit intracortical activity. IEEE Trans Biomed Eng 1988;35(9):719–32.

Grattarola M, Martionoia S. Modelling the neuron–microtransducer junction: from extracellular to patch recording. IEEE Trans Biomed Eng 1993;40(1):35–41.

Gross GW. Internal dynamics of randomized mammalian neuronal networks in culture. In: Stenger DA, McKenna TM, editors. Enabling Technologies for Cultured Neural Networks. New York: Academic Press, 1994:277–317.

Hodgkin AL, Huxley AF. A quantitative description of membrane current and its application to conduction and excitation in nerve. J Phys 1952;117:500–44.

Holt GR, Koch C. Electrical interactions via the extracellular potential near cell bodies. J Comput Neurosci 1999;6:169–84.

James CD, Davis R, Meyer M, Turner A, Turner S, Wither G, Kam L, Banker G, Craighead H, Isaacson M, Turner J, Shain W. Aligned microcontact printing of micrometer-scale poly-L-lysine structures for controlled growth of cultured neurons on planar microelectrode arrays. IEEE Trans Biomed Eng 2000;47(1):17–21.

Ketchum KL, Haberly LB. Membrane currents evoked by afferent fiber stimulation in rat piriform cortex. I. Current source-density analysis. J Neurophysiol 1993;69(1):248–60.

Koch C, Segev I, editors.Methods in Neural Modeling: From Ions to Networks. Cambridge, MA: MIT Press, 1998.

Maher MP, Pine J, Wright J, Tai YC. The neurochip: a new multielectrode device for stimulating and recording from cultured neurons. J Neurosci Methods 1999;87(1):45–56.

Nadásdy Z, Hirase H, Czurkó A, Csicsvari J, Buzsaki G. Replay and time compression of recurring spike sequences in the hippocampus. J Neurosci 1999;19(21):9497–507.

Nicholson C, Freeman JA. Theory of current source-density analysis and determination of conductivity tensor for anuram cerebellum. J Neurophysiol 1975;38(2):356–68.

Novak JL, Wheeler BC. Two-dimensional current source density analysis of propagation delays for components of epileptiform bursts in rat hippocampal slices. Brain Res 1989;497(2):223–30.

Nuñez P. Electric Field of the Brain: The Neurophysics of EEG. New York: Oxford University Press, 1981.

Oka H, Shimono K, Ogawa R, Sugihara H, Taketani M. A new planar multielectrode array for extracelullar recording: application to hippocampal acute slice. J Neurosci Methods 1999;93:61–7.

Pine J. Recording action potentials from cultured neurons with extracellular microcircuit electrodes. J Neurosci Methods 1980;2(1):19–31.

Quirk MC, Blum KI, Wilson MA. Experience-dependent changes in extracellular spike amplitude may reflect regulation of dendritic action potential back-propagation in rat hippocampal pyramidal cells. J Neurosci 2001;21(1):240–8.

Rae J, Cooper K, Gates P, Watsky M. Low access resistance perforated patch recordings using amphotericin B. J Neurosci Methods 1991;37:15–26.

Rall W. Distributions of potential in cylindrical coordinates and time constants for a membrane cylinder. Biophys J 1969;9:1509–41.

Rapp M, Yarom Y, Segev I. Modelling back propagating action potential in weakly excitable dendrites of neocortical pyramidal cells. Proc Natl Acad Sci USA 1996;93:11985–90.

Regehr WG, Pine J, Cohan CS, Mischke MD, Tank DW. Sealing cultured invertebrate neurons to embedded dish electrodes facilities long-term stimulation and recording. J Neurosci Methods 1989;30:91–106.

Traub RD, Wong RKS, Miles R, Michelson H. A model of a CA3 hippocampal pyramidal neuron incorporating voltage-clamp data on intrinsic conductances. J Neurophys 1991;66(2):635–50.

Zeck G, Fromherz P. Noninvasive neuroelectronic interfacing with synaptically connected snail neurons immobilized on a semiconductor chip. Proc Natl Acad Sci USA 2001;98(18):10457–62.